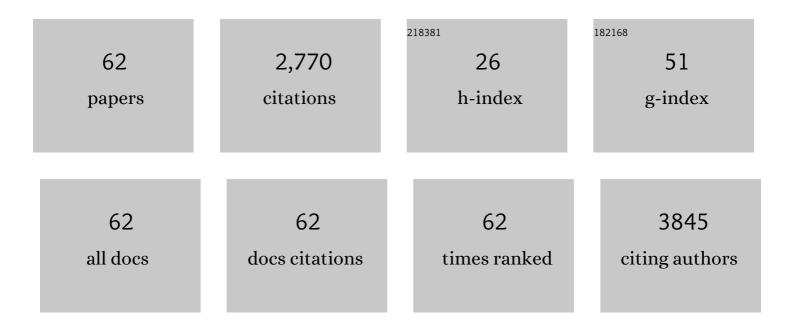


## List of Publications by Year in descending order

Source: https://exaly.com/author-pdf/7368206/publications.pdf Version: 2024-02-01



DONGLI

#	Article	IF	CITATIONS
1	3D Printable Graphene Composite. Scientific Reports, 2015, 5, 11181.	1.6	337
2	Two-dimensional non-volatile programmable p–n junctions. Nature Nanotechnology, 2017, 12, 901-906.	15.6	278
3	Self-Powered Broad-band Photodetectors Based on Vertically Stacked WSe <sub>2</sub> /Bi <sub>2</sub> Te <sub>3</sub> <i>p–n</i> Heterojunctions. ACS Nano, 2019, 13, 13573-13580.	7.3	165
4	Subâ€Thick Electrodes with Enhanced Transport Kinetics via In Situ Epitaxial Heterogeneous Interfaces for High Areal apacity Lithium Ion Batteries. Small, 2021, 17, e2100778.	5.2	141
5	Band Alignment Engineering in Two-Dimensional Lateral Heterostructures. Journal of the American Chemical Society, 2018, 140, 11193-11197.	6.6	136
6	Nonvolatile Floatingâ€Gate Memories Based on Stacked Black Phosphorus–Boron Nitride–MoS <sub>2</sub> Heterostructures. Advanced Functional Materials, 2015, 25, 7360-7365.	7.8	129
7	Van der Waals epitaxial growth of vertically stacked Sb2Te3/MoS2 p–n heterojunctions for high performance optoelectronics. Nano Energy, 2019, 59, 66-74.	8.2	112
8	Highly stable lead-free Cs3Bi2I9 perovskite nanoplates for photodetection applications. Nano Research, 2019, 12, 1894-1899.	5.8	96
9	Floating-Gate Manipulated Graphene-Black Phosphorus Heterojunction for Nonvolatile Ambipolar Schottky Junction Memories, Memory Inverter Circuits, and Logic Rectifiers. Nano Letters, 2017, 17, 6353-6359.	4.5	87
10	Gateâ€Controlled BP–WSe <sub>2</sub> Heterojunction Diode for Logic Rectifiers and Logic Optoelectronics. Small, 2017, 13, 1603726.	5.2	86
11	Rational Kinetics Control toward Universal Growth of 2D Vertically Stacked Heterostructures. Advanced Materials, 2019, 31, e1901351.	11.1	79
12	Liquid-Metal-Assisted Growth of Vertical GaSe/MoS <sub>2</sub> p–n Heterojunctions for Sensitive Self-Driven Photodetectors. ACS Nano, 2021, 15, 10039-10047.	7.3	73
13	WO <sub>3</sub> –WS <sub>2</sub> Vertical Bilayer Heterostructures with High Photoluminescence Quantum Yield. Journal of the American Chemical Society, 2019, 141, 11754-11758.	6.6	69
14	Ultrahigh-Performance Optoelectronics Demonstrated in Ultrathin Perovskite-Based Vertical Semiconductor Heterostructures. ACS Nano, 2019, 13, 7996-8003.	7.3	64
15	High-performance optoelectronic devices based on van der Waals vertical MoS2/MoSe2 heterostructures. Nano Research, 2020, 13, 1053-1059.	5.8	63
16	Facile Synthesis of Na-Doped MnO <sub>2</sub> Nanosheets on Carbon Nanotube Fibers for Ultrahigh-Energy-Density All-Solid-State Wearable Asymmetric Supercapacitors. ACS Applied Materials & Interfaces, 2018, 10, 37233-37241.	4.0	60
17	Tandem gasochromic-Pd-WO3/graphene/Si device for room-temperature high-performance optoelectronic hydrogen sensors. Carbon, 2018, 130, 281-287.	5.4	56
18	Nonvolatile MoTe <sub>2</sub> <i>p–n</i> Diodes for Optoelectronic Logics. ACS Nano, 2019, 13, 7216-7222.	7.3	52

Dong Li

#	Article	IF	CITATIONS
19	High-responsivity two-dimensional p-Pbl <sub>2</sub> /n-WS <sub>2</sub> vertical heterostructure photodetectors enhanced by photogating effect. Materials Horizons, 2019, 6, 1474-1480.	6.4	51
20	Probing and Manipulating Carrier Interlayer Diffusion in van der Waals Multilayer by Constructing Type-I Heterostructure. Nano Letters, 2019, 19, 7217-7225.	4.5	42
21	Epitaxial synthesis of ultrathin β-In <sub>2</sub> Se <sub>3</sub> /MoS <sub>2</sub> heterostructures with high visible/near-infrared photoresponse. Nanoscale, 2020, 12, 6480-6488.	2.8	42
22	Doubleâ€Gate MoS <sub>2</sub> Fieldâ€Effect Transistors with Fullâ€Range Tunable Threshold Voltage for Multifunctional Logic Circuits. Advanced Materials, 2021, 33, e2101036.	11.1	42
23	Recent Advances in Twoâ€Dimensional Heterostructures: From Band Alignment Engineering to Advanced Optoelectronic Applications. Advanced Electronic Materials, 2021, 7, 2001174.	2.6	34
24	Dualâ€channel type tunable fieldâ€effect transistors based on vertical bilayer WS <sub>2(1 â^' <i>x</i>)</sub> Se <sub>2<i>x</i></sub> /SnS <sub>2</sub> heterostructures. Informa Materiály, 2020, 2, 752-760.	Änsã5	32
25	Tunable bandgap in few-layer black phosphorus by electrical field. 2D Materials, 2017, 4, 031009.	2.0	30
26	Light-triggered two-dimensional lateral homogeneous p-n diodes for opto-electrical interconnection circuits. Science Bulletin, 2020, 65, 293-299.	4.3	29
27	Direct Growth of Nanocrystalline Graphene/Graphite Transparent Electrodes on Si/SiO <sub>2</sub> for Metalâ€Free Schottky Junction Photodetectors. Advanced Functional Materials, 2014, 24, 835-840.	7.8	28
28	Growth of CdSe/MoS2 vertical heterostructures for fast visible-wavelength photodetectors. Journal of Alloys and Compounds, 2020, 815, 152309.	2.8	27
29	Floating-gate controlled programmable non-volatile black phosphorus PNP junction memory. Nanoscale, 2018, 10, 3148-3152.	2.8	22
30	Efficient control of emission and carrier polarity in WS2 monolayer by indium doping. Science China Materials, 2021, 64, 1449-1456.	3.5	21
31	Plasmonically engineered light-matter interactions in Au-nanoparticle/MoS2 heterostructures for artificial optoelectronic synapse. Nano Research, 2022, 15, 3539-3547.	5.8	20
32	Light-triggered interfacial charge transfer and enhanced photodetection in CdSe/ZnS quantum dots/MoS <sub>2</sub> mixed-dimensional phototransistors. Opto-Electronic Advances, 2021, 4, 210017-210017.	6.4	19
33	Vapor growth of CdS nanowires/WS <sub>2</sub> nanosheet heterostructures with sensitive photodetections. Nanotechnology, 2019, 30, 345603.	1.3	18
34	Magnetic Doping Induced Strong Circularly Polarized Light Emission and Detection in 2D Layered Halide Perovskite. Advanced Optical Materials, 2022, 10, .	3.6	17
35	Photo-Induced Doping in Graphene/Silicon Heterostructures. Journal of Physical Chemistry C, 2015, 119, 1061-1066.	1.5	16
36	Tight-binding model for electronic structure of hexagonal boron phosphide monolayer and bilayer. Journal of Physics Condensed Matter, 2019, 31, 285501.	0.7	14

Dong Li

#	Article	IF	CITATIONS
37	Direct Growth of Nanographene on Silicon with Thin Oxide Layer for Highâ€Performance Nanographeneâ€Oxideâ€Silicon Diodes. Advanced Functional Materials, 2014, 24, 7613-7618.	7.8	13
38	Trion-Induced Distinct Transient Behavior and Stokes Shift in WS <sub>2</sub> Monolayers. Journal of Physical Chemistry Letters, 2019, 10, 3763-3772.	2.1	13
39	Record high photoresponse observed in CdS-black phosphorous van der Waals heterojunction photodiode. Science China Materials, 2020, 63, 1570-1578.	3.5	13
40	Contact and injection engineering for low SS reconfigurable FETs and high gain complementary inverters. Science Bulletin, 2020, 65, 2007-2013.	4.3	13
41	Electrically tunable large magnetoresistance in graphene/silicon Schottky junctions. Carbon, 2017, 123, 106-111.	5.4	12
42	Direct growth of nanocrystalline graphene/graphite all carbon transparent electrode for graphene glass and photodetectors. Carbon, 2017, 111, 1-7.	5.4	12
43	Controlled growth of SnSe/MoS <sub>2</sub> vertical p–n heterojunction for optoelectronic applications. Nano Futures, 2021, 5, 015002.	1.0	12
44	Stress- and electric-field-induced band gap tuning in hexagonal boron phosphide layers. Journal of Physics Condensed Matter, 2019, 31, 465502.	0.7	10
45	Magnetic-brightening and control of dark exciton in CsPbBr3 perovskite. Science China Materials, 2020, 63, 1503-1509.	3.5	8
46	A novel visible light sensing and recording system enabled by integration of photodetector and electrochromic devices. Nanoscale, 2021, 13, 9177-9184.	2.8	8
47	Polar-Induced Selective Epitaxial Growth of Multijunction Nanoribbons for High-Performance Optoelectronics. ACS Applied Materials & Interfaces, 2019, 11, 15813-15820.	4.0	7
48	Study on the graphene/silicon Schottky diodes by transferring graphene transparent electrodes on silicon. Thin Solid Films, 2015, 592, 281-286.	0.8	6
49	Revealing the many-body interactions and valley-polarization behavior in Re-doped MoS2 monolayers. Applied Physics Letters, 2021, 118, .	1.5	6
50	Strain-controlled synthesis of ultrathin hexagonal GaTe/MoS2 heterostructure for sensitive photodetection. IScience, 2021, 24, 103031.	1.9	6
51	Manipulating Picosecond Photoresponse in van der Waals Heterostructure Photodetectors. Advanced Functional Materials, 2022, 32, .	7.8	6
52	Morphology Deformation and Giant Electronic Band Modulation in Long-Wavelength WS <sub>2</sub> Moiré Superlattices. Nano Letters, 2022, 22, 5997-6003.	4.5	6
53	Bottom-up fabrication of semiconducting 2D coordination nanosheets for versatile bioimaging and photodetecting applications. Materials Advances, 2021, 2, 5189-5194.	2.6	5
54	Strong interfacial coupling in vertical WSe2/WS2 heterostructure for high performance photodetection. Applied Physics Letters, 2022, 120, .	1.5	5

Dong Li

#	Article	lF	CITATIONS
55	Thermal annealing and air exposing effect on the graphene/silicon Schottky junctions. Solid State Communications, 2015, 201, 115-119.	0.9	4
56	Novel p-n junctions based on ambipolar two-dimensional crystals. Wuli Xuebao/Acta Physica Sinica, 2017, 66, 217302.	0.2	4
57	Facile fabrication of a single-particle platform with high throughput via substrate surface potential regulated large-spacing nanoparticle assembly. Nano Research, 0, , 1.	5.8	4
58	Solution-processed anchoring zinc oxide quantum dots on covalently modified graphene oxide. Journal of Nanoparticle Research, 2014, 16, 1.	0.8	3
59	Picosecond electrical response in graphene/MoTe2 heterojunction with high responsivity in the near infrared region. Fundamental Research, 2022, 2, 405-411.	1.6	3
60	Gallium doping-assisted giant photoluminescence enhancement of monolayer MoS <sub>2</sub> grown by chemical vapor deposition. Applied Physics Letters, 2022, 120, 221902.	1.5	2
61	Band Alignment Engineering by Twist Angle and Composition Modulation for Heterobilayer. Small, 2022, 18, .	5.2	2
62	Controlled Synthesis of Ultrathin Hexagonal-GaTe on MoS <sub>2</sub> Via Strain Engineering. SSRN Electronic Journal, 0, , .	0.4	0